Available online at www.sciencedirect.com

SciVerse ScienceDirect

Ceramics International 38 (2012) 2495–2500

CERAMICS INTERNATIONAL

www.elsevier.com/locate/ceramint

# Preparation of low cost glass–ceramics from molten blast furnace slag

Yan Zhao [a], Dengfu Chen [a,*], Yanyan Bi [b], Mujun Long [a]

[a] Laboratory of Metallurgy and Materials, College of Materials Science and Engineering, Chongqing University, Chongqing 400030, China
[b] Department of Materials Science and Engineering, Royal Institute of Technology, Stockholm 10044, Sweden

Received 8 October 2011; received in revised form 4 November 2011; accepted 5 November 2011
Available online 11 November 2011

---

## Abstract

In the current paper, a low-cost technology was used to prepare glass–ceramics through directly heat-treating with molten glass containing blast furnace slag and silica sand. By making use of the sensible heat of the molten slag, the energy cost was much lower than that in conventional method. The utilized ratio of slag was about 90% and the optimum heat treatment schedule for glass–ceramics was confirmed by an $L_9(3^4)$ orthogonal test. The effect of $CaF_2$ on the microstructure of the glass–ceramics was studied by DSC, XRD and SEM, the bending strength of the glass–ceramics was tested by three points bending tester. The results showed that, after the optimum heat treatment schedule of nucleation at 780 °C for 0.5 h and crystallization at 960 °C for 1.5 h, the crystalline phases were akermanite and diopside, the bending strength of the glass–ceramics was about 45.8 MPa. If $CaF_2$ was added, a remarkable reduction of crystal size was observed, the crystallization of diopside and $Ca_2SiO_2F_2$ was promoted while that of akermanite was inhibited, the bending strength of glass–ceramics samples could be greatly improved to 120 MPa.

*Keywords:* B. Microstructure-final; C. Mechanical properties; D. Glass–ceramics; Molten blast furnace slag

---

## 1. Instruction

Blast furnace slag is a major waste produced by iron and steel industry, which is also a valuable resource for recycling and utilizing. The slag is usually quenched from 1450 °C, and subsequently used for cement and concrete as raw materials, which usually has low values. Air, water and dust emission pollutions resulting from these processes and the loss of huge amount of sensible heat in molten slag should be worthy of concern as well [1,2]. Consequently, how to save the heat energy in molten slag and convert slag into more valuable and environment friendly products is a new focus across the world these years.

The mechanical properties of glass–ceramics are superior to granite and marble as construction materials, and glass–ceramics also exhibit other excellent properties which are beneficial for particular applications, as exemplified by high strength, good thermal shock resistance and low expansion. There have been considerable research on the preparation of glass–ceramics from industrial waste since 1970s, which includes melting [3–6], sintering [7–12] and petrurgic methods [13,14]. The melting and sintering methods, called conventional method, are to develop glass–ceramics by a two-stage heat treatment process. The raw materials are quenched from molten state to room temperature firstly, and then the parent glass is re-heated to two holding stages at high temperatures for internal nucleation and crystallization. However, the procedures are highly energy-consuming. The petrurgic method is to develop glass–ceramics by a controlled, usually very slow, cooling of the parent glass from its molten state without a hold at an intermediate temperature, both nucleation and crystallization can take place during the cooling process. The petrurgic method is more economical than the conventional method, because it avoids the re-heating process of raw materials. Nevertheless, the cooling process usually needs to be controlled accurately and very slowly, so it is very difficult for industrial production and very little detailed work has reported on this method [13]. According to physics and chemistry theory of silicate, the crystalline phase has the lowest free energy, so molten glass will undergo nucleation and crystallization depending on undercooling if it is placed at a lower temperature than its melting point (it also may be a temperature range) for certain periods of time. So the method dealing with molten glass at a suitable

---

* Corresponding author. Tel.: +86 23 65102467.
*E-mail address:* chendfu@cqu.edu.cn (D. Chen).

doi:10.1016/j.ceramint.2011.11.018

temperature directly for certain period also can prepare glass–ceramics and will significantly reduce the energy consumption or cost compared with conventional method. However, the nucleation and crystallization behavior in molten glass may be different from consequences in the research of conventional glass–ceramics preparation because of different heat treatment conditions, which was investigated in detail in the present paper.

The primary aim of the present study is to determine a low cost way to prepare glass–ceramics from molten blast furnace slag, including the composition and heat treatment schedule. The crystallization behavior of the glass and the influence of $CaF_2$ on its microstructure during the process is also studied by differential scanning calorimetry (DSC), scanning electron microscope (SEM) and X-ray diffraction analysis (XRD).

## 2. Experimental procedure

### 2.1. Raw materials and glass–ceramics forming

The blast furnace slag used in this work was provided by Chongqing Iron and Steel Company. The chemical composition of the slag is summarized in Table 1. In order to design the $CaO–Al_2O_3–SiO_2–MgO$ glass–ceramics, silica sand powder was added during the process. $CaF_2$ was added as a nucleation agent after the heat treatment schedule was determined, in attempt to promote the crystallization and improve performance of glass–ceramics. The method of preparation of glass–ceramics in present study is illustrated in Fig. 1.

As shown in Fig. 1, the mixed materials were melted in a graphite crucible at 1500–1600 °C with an induction furnace. After complete melting, the molten glass was cast into a preheated steel mould for 1–2 min to make sure the surface solidify, and then the sample was directly put into an electric furnace with a holding temperature for nucleation and followed by a higher holding temperature for crystallization. Finally, the resultant glass–ceramics sample was got after annealing.

### 2.2. Differential scanning calorimetry analysis

The heat variations during phase transformations were analyzed by DSC (NETZSCH STA449C Thermal Analyzer). 30 mg of glass sample was put in a flowing atmosphere of nitrogen, and alumina powder was used as a reference material within the temperature range of 20–1400 °C at a heating rate of 20 °C/min. DSC was employed to determine the glass transition temperature and crystallization peak temperature.

### 2.3. X-ray diffraction analysis

X-ray diffraction was performed by D/Max-1200X diffractometer using Cu Kα, operated at 40 kV and 35 mA and in the $2\theta$ range from 10° to 90° at a rate of 4°/min. The crystalline phases were identified by comparing the peak intensities and positions with those in the Joint Committee on Powder Diffraction Standards (JCPDS) data files. XRD was used to identify the crystalline phases in the final glass–ceramics.

Table 1
Compositions of blast furnace slag (wt%).

| Oxide | CaO | MgO | $Al_2O_3$ | $SiO_2$ | FeO | MnO | $TiO_2$ |
|---|---|---|---|---|---|---|---|
| Amount | 38.09 | 9.64 | 14.45 | 33.41 | 0.38 | 0.56 | 3.09 |

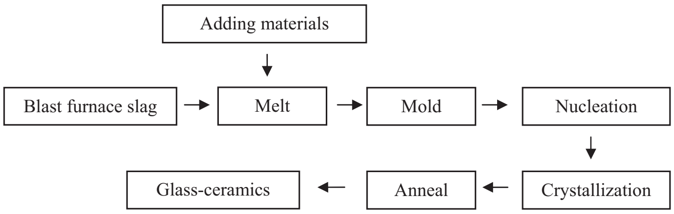

Fig. 1. Flow chart of glass–ceramics preparation method.

### 2.4. Microstructure characterization

The surfaces of selected samples were corroded in HF (3 vol%) for 10 s and then the microstructure was investigated by FEI Nova Nano SEM 400. SEM was carried out to analyze the morphology of crystals in the final glass–ceramics.

### 2.5. Measurements of mechanical properties

Three point bending test was performed in an Electronic Universal Tester. The size of glass–ceramics sample was length 8 cm × width 4 cm × height 2 cm. This was used to measure the bending strength of the final glass–ceramics.

## 3. Result and discussion

### 3.1. Composition designed of glass–ceramics

In order to utilize slag as much as possible and ensure the excellent property of glass–ceramics, series of melilite and pyroxene phases were selected as the major phases, which suggested 5–15 wt% silica sand was added according to the

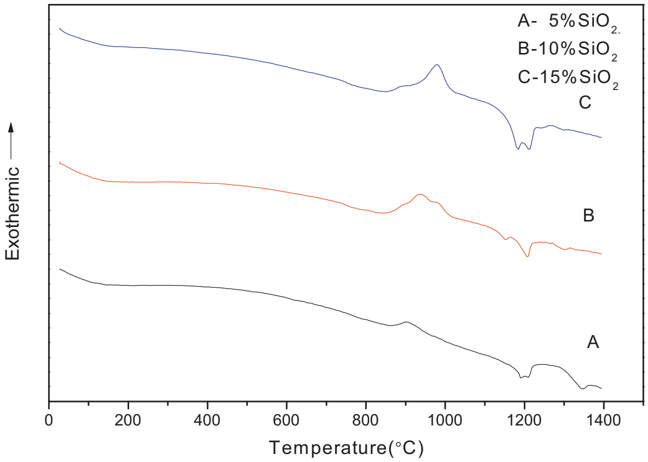

Fig. 2. Differential scanning calorimetry analysis curves of glass with different amount of $SiO_2$.

Table 2
Chemical composition of investigated glass (wt%).

| | Blast furnace slag | $SiO_2$ | $CaF_2$ |
|---|---|---|---|
| S1 | 90.9 | 9.1 | – |
| S2 | 88.5 | 8.8 | 2.7 |
| S3 | 86.2 | 8.6 | 5.2 |
| S4 | 84.0 | 8.4 | 7.6 |

Table 3
Orthogonal table of experimental factors.

| Level | Nucleation temperature (°C) | Crystallization temperature (°C) | Nucleation time (h) | Crystallization time (h) |
|---|---|---|---|---|
| 1 | 780 | 920 | 0.5 | 0.5 |
| 2 | 800 | 940 | 1 | 1 |
| 3 | 820 | 960 | 1.5 | 1.5 |

$CaO–Al_2O_3–SiO_2–MgO$ phase diagram. In this paper, 5 wt%, 10 wt% and 15 wt% silica sand powder was added separately to be monitored the crystallization efficiency by DSC. Fig. 2 shows the DSC curves of three glass samples. A sample with 5 wt% silica sand addition has a small exothermic peak, while B and C samples containing 10 wt% and 15 wt% separately, have broad and obvious exothermic peaks, which indicate the excellent crystallization ability. Therefore, B sample with 10 wt% silica sand addition is employed for the lowest cost glass–ceramics composition. With the aim of investigating the influence of $CaF_2$ on the crystallization behavior, different amounts of $CaF_2$ were added. Table 2 shows the different compositions of glass–ceramics.

### 3.2. Determination of the optimum heat treatment schedule

Fig. 3 shows the DSC curve of S1 glass. The small endothermic peak (760 °C) indicates the glass transition temperature, so the optimum nucleation temperature was determined at 20–60 °C higher than glass transition temperature [15]. The exothermic peak (940 °C) corresponds to the optimal crystallization temperature of S1 glass. A sharp endothermic peak appears at 1200 °C, suggesting some crystals have molten.

The optimum heat treatment schedule for S1 glass was determined by a $L_9(3^4)$ orthogonal test. Table 3 shows the experimental conditions for the heat treatment. Table 4 lists the results of $L_9(3^4)$ test and the bending strength of different samples with different heat treatment schedules. As summarized in Table 4, the influence to bending strength decreases in the order of crystallization temperature > crystallization time - > nucleation temperature > nucleation time. The bending strength of S1(3) is the highest, 45.8 MPa. Therefore, the optimum heat treatment schedule was determined as nucleation at 780 °C for 0.5 h and crystallization at 960 °C for 1.5 h.

Table 4
Scheme of heat treatment and quality of different samples.

| | Nucleation temperature (°C) | Crystallization temperature (°C) | Nucleation time (h) | Crystallization time (h) | Bending strength (MPa) |
|---|---|---|---|---|---|
| S1(1) | 780 | 920 | 1.5 | 1 | 13.5 |
| S1(2) | 780 | 940 | 1 | 0.5 | 16.6 |
| S1(3) | 780 | 960 | 0.5 | 1.5 | 45.8 |
| S1(4) | 800 | 920 | 0.5 | 0.5 | 17.8 |
| S1(5) | 800 | 940 | 1.5 | 1.5 | 21.0 |
| S1(6) | 800 | 960 | 1 | 1 | 31.2 |
| S1(7) | 820 | 920 | 1 | 1.5 | 41.8 |
| S1(8) | 820 | 940 | 0.5 | 1 | 15.8 |
| S1(9) | 820 | 960 | 1.5 | 0.5 | 31.9 |
| Range | 4.666 | 14.143 | 5.778 | 11.854 | |

### 3.3. The XRD analysis for final glass–ceramics

Fig. 4 shows the XRD diffraction patterns of S1(3), S1(4), S2, S3 and S4 samples. S2, S3 and S4 with different amounts of $CaF_2$ were prepared as the heat treatment schedule determined above. Fig. 4 indicates that akermanite and diopside are the major crystal phases in these samples. During the crystallization process, alkali

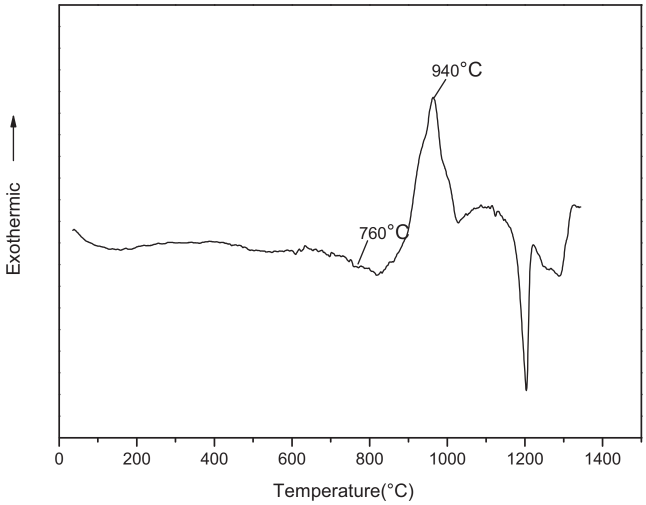

Fig. 3. Differential scanning calorimetry analysis curve of S1 glass.

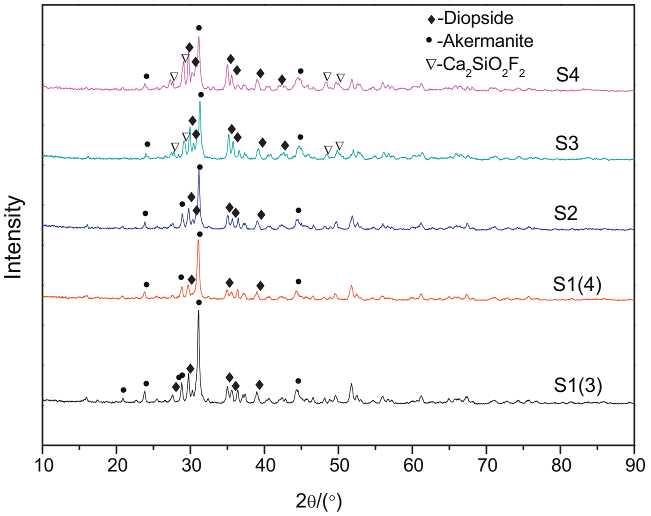

Fig. 4. X-ray diffraction patterns of glass–ceramics.

oxides damaged the network of glass and decreased the proportion of bridge oxygen, thus induced the transformation of octahedral magnesium groups $[MgO_6]^{10-}$ into tetrahedral groups $[MgO_4]^{6-}$. $[Si_2O_7]^{6-}$ favored combining with $[MgO_4]^{6-}$ and akermanite ($Ca_2MgSi_2O_7$) formed as a result. The remajoring octahedrons tended to combine with $[CaO_6]^{10-}$ and $[SiO_3]^{2-}$, and leaded to the formation of diopside ($CaMgSi_2O_6$) [16].

As illustrated in Fig. 4, there are more diffraction peaks with higher peak intensity in S1(3) than that in S1(4), indicating

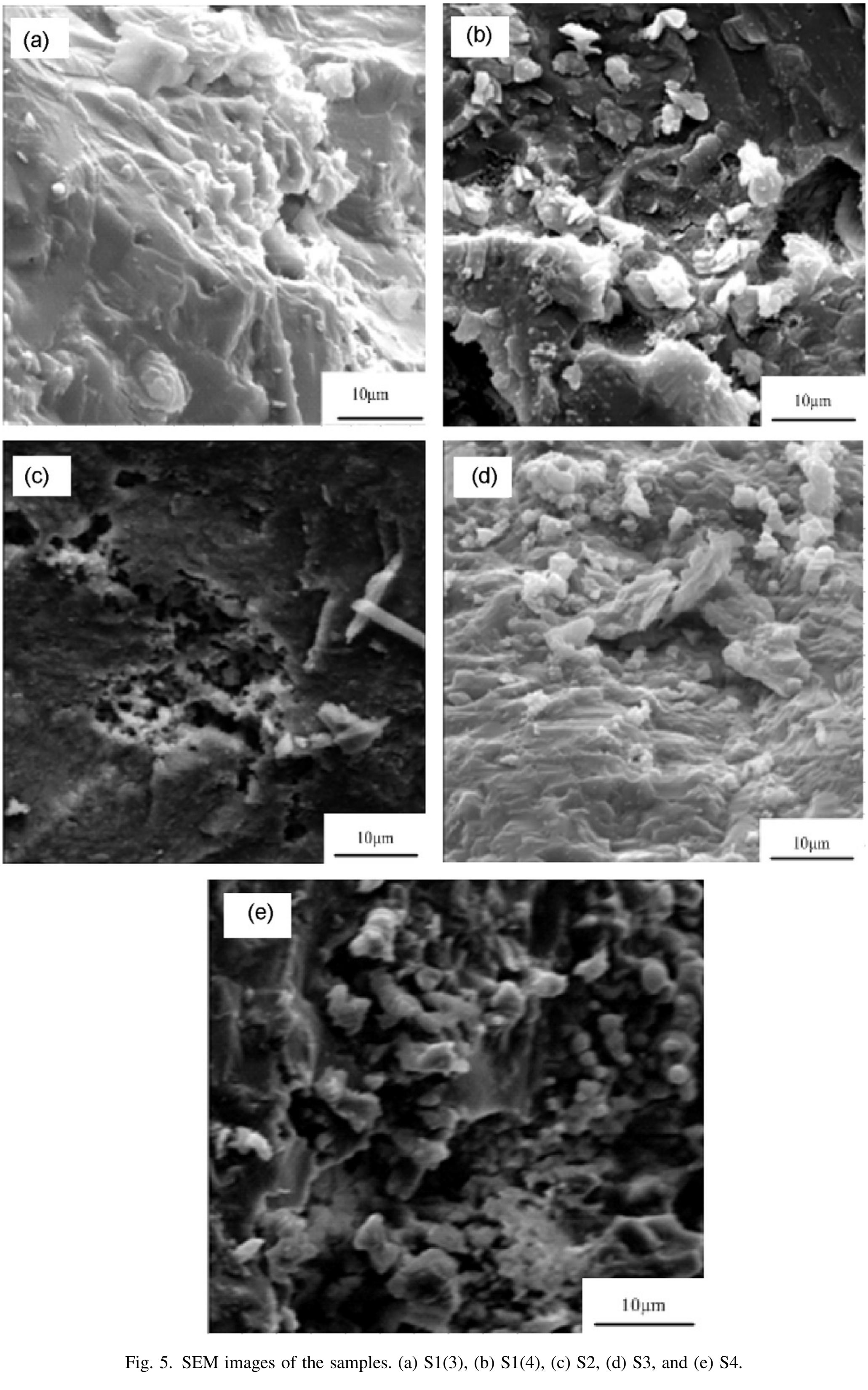

Fig. 5. SEM images of the samples. (a) S1(3), (b) S1(4), (c) S2, (d) S3, and (e) S4.

S1(3) contains more crystalline phases than S1(4). As a result, the strength of S1(3) is higher than S1(4), which has been supported by the strength test results. As shown in Fig. 4 and compared to S1(3), the amount of diopside increases and $Ca_2SiO_2F_2$ is beginning to appear together with the appreciable disappearance of some akermanite in S2, S3 and S4. This is because, $F^-$ ions replaced $O^{2-}$ ions in $[SiO_4]^{4-}$, which induced the formation of $[SiO_2F_2]^{4-}$ and more free $O^{2-}$ ions, thus the $Ca_2SiO_2F_2$ phase appeared. At the same time, another reaction occurred as following:

$$[Si_2O_7]^{6-} + O^{2-} = [SiO_4]^{4-} + [SiO_4]^{4-} \quad (1)$$

Through this reaction, the amount of $[Si_2O_7]^{6-}$ ion clusters decreased, causing some akermanite crystals disappear. More $[SiO_4]^{4-}$ ion clusters combined into chain structural $[Si_2O_6]^{4-}$ through bridge oxygen, so more diopside crystals appeared. Hoda found that the addition of $CaF_2$ could decrease the crystallization activation energy of glass–ceramics, and make the structure transform from layer to chain and more diopside crystals formed, which compares extremely favorably with our results [17].

### 3.4. The SEM analysis for final glass–ceramics

Fig. 5 reveals SEM images of different samples. As seen in Fig. 5(a) and (b), it is clear that the crystals are denser in S1(3), and amorphous phase takes a larger proportion in S1(4), which may result in lower bending strength. The analysis result is also supported by evidence from XRD and bending strength test. Fig. 5(c)–(e), indicate that more and smaller spherical crystals have formed accompanying by more $CaF_2$ adding. Fig. 5(e) shows the microstructure of S4 containing 7.6 wt% is composed of ultrafine crystalline grains with size of 2–5 μm randomly distributed in the glassy matrix. This is because that, $F^-$ ions played the nuclear role and generated large amount of nucleus in glass, nucleus kept interacting when they were growing into crystals, so the grain size would become smaller [18].

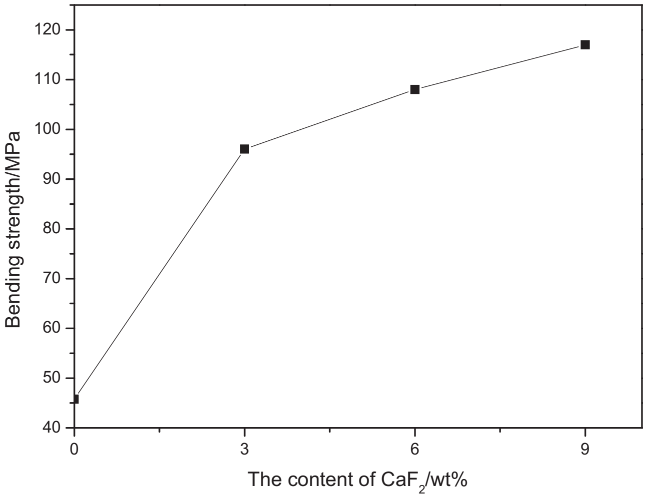

Fig. 6. The bending strength of glass–ceramics with different amount of $CaF_2$.

### 3.5. The bending strength analysis for final glass–ceramics

Fig. 6 shows the bending strength of glass–ceramics samples with different amount of $CaF_2$ addition. By increasing the amount of $CaF_2$, the bending strength of samples trends to increase, up to 120 MPa in S4. According to Griffith's consequence, the possible explanation is that the addition of $CaF_2$ decreased crystal size and produced more crystals, so cracks were difficult to generate or extend in these samples containing more and smaller crystals. The addition of $CaF_2$ significantly improved the bending strength of glass–ceramics samples, which was consistent with a previous work carried out with conventional method by Guo and Yang [19].

## 4. Conclusion

The study highlighted a method of preparing glass–ceramics that processed directly heat treatment to molten blast furnace slag rather than glass at room temperature. Obviously, it promised lower energy consumption than conventional method. Glass–ceramics were successfully synthesized from molten blast furnace slag with about 10 wt% silica sand addition through the method. The utilization ratio of blast-furnace slag was up to about 90 wt%, which promised less raw materials cost.

The molten glass could be converted into glass–ceramics after a suitable two-stage nucleation–crystallization process. The optimum heat treatment schedule was confirmed as nucleation at 780 °C for 0.5 h and crystallization at 960 °C for 1.5 h with a $L_9(3^4)$ orthogonal test. The major crystalline phases were akermanite and diopside, and the bending strength of the sample reached 45.8 MPa.

With the increase of the amount $CaF_2$, a remarkable reduction of crystal size was observed, the devitrification of diopside and $Ca_2SiO_2F_2$ was promoted while akermanite decreased. The strength of glass–ceramics samples were also improved, up to 120 MPa when 7.6% $CaF_2$ was added.

This method will be an excellent way to deal with blast furnace slag in iron and steel industry if the product line as this method connects with blast furnace directly, which will generate large amount of economic benefits.

## Acknowledgement

The authors would like to thank the Natural Science Foundation of China (NSFC) for the financial support.

## References

[1] D. Chen, X. Zuo, L. Wen, L. Dong, G. Qiu, Methods and problems of heat recovery from molten blast furnace slag, Techniques and Equipment for Environmental Pollution Control 7 (7) (2006) 133–137 (in Chinese).

[2] V. Gomes, C.D.G. De Borba, H.G. Riella, Production and characterization of glass ceramics from steelwork slag, Journal of Materials Science 37 (12) (2002) 2581–2585.

[3] M. Rezvani, B. Eftekhari, M. Solati-Hashjin, V.K. Marghussian, Effect of $Cr_2O_3$, $Fe_2O_3$ and $TiO_2$ nucleants on the crystallization behavior of $SiO_2$–$Al_2O_3$–CaO–MgO($R_2O$) glass–ceramics, Ceramics International 31 (1) (2005) 75–80.

[4] M. Mirsaneh, I.M. Reaney, P.V. Hatton, S. Bhakta, P.F. James, Effect of $P_2O_5$ on the early stage crystallization of K-fluorrichterite glass–ceramics, Journal of Non-Crystalline Solids 354 (28) (2008) 3362–3368.

[5] S.N. Salama, E.A. Saad, H. Darwish, H.A. Abo-Mosallam, Formation of glass–ceramic materials based on pyroxene solid solution-fluorapatite phases and their thermal expansion properties, Ceramics International 31 (4) (2005) 559–566.

[6] J. Yang, D. Zhang, J. Hou, B. He, X. Bo, Preparation of glass–ceramics from red mud in the aluminium industries, Ceramics International 34 (1) (2008) 125–130.

[7] A.A. Francis, Conversion of blast furnace slag into new glass–ceramics material, Journal of the European Ceramic Society 24 (9) (2004) 2819–2824.

[8] H. Motz, J. Geiseler, Products of steel slags an opportunity to save natural resources, Waste Management 21 (3) (2001) 285–293.

[9] S. Ghosh, M. Das, S. Chakrabarti, et al., Development of ceramic tiles from common clay and blast furnace slag, Ceramics International 28 (3) (2002) 393–400.

[10] S. Zhang, Q. Yue, H. Yu, J. Xie, X. Wang, Preparation of glass–ceramics produced from blast-furnace slag, Journal of Shandong University (Natural Science) 41 (05) (2006) 129–133 (in Chinese).

[11] H. Liu, H. Lu, D. Chen, H. Wang, H. Xu, R. Zhang, Preparation and properties of glass–ceramics derived from blast-furnace slag by a ceramic-sintering process, Ceramics International 35 (8) (2009) 3181–3184.

[12] A. Karamanov, T. Giuliana, M. Pelino, Iron-rich sintered glass–ceramics from industry wastes, Journal of the European Ceramic Society 82 (11) (1999) 3012–3016.

[13] R.D. Rawlings, J.P. Wu, A.R. Boccaccini, Glass–ceramics: their production from wastes – a review, Journal of Materials Science 41 (3) (2006) 733–761.

[14] A.A. Francis, R.D. Rawlings, A.R. Boccaccini, Glass–ceramics from mixtures of coal ash and soda-lime glass by the petrurgic method, Journal of Materials Science Letters 21 (12) (2002) 975–980.

[15] S. Likitvanichkul, W.C. Lacourse, Effect of fluorine content on crystallization of canasite glass–ceramics, Journal of Materials Science 30 (24) (1995) 6151–6155.

[16] D.U. Tulyaganov, M.J. Ribeiro, J.A. Labrincha, Development of glass–ceramics by sintering and crystallization of fine powders of calcium–magnesium–aluminosilicate glass, Ceramics International 28 (5) (2002) 515–520.

[17] S.N. Hoda, G.H. Beall, Advances in nucleation and crystallization in glasses, American Ceramic Society 04 (1982) 287–291.

[18] H. Fathi, A. Johnson, R. van Noort, J.M. Ward, I.M. Brook, The effect of calcium fluoride ($CaF_2$) on the chemical solubility of an apatite–mullite glass–ceramics material, Dental Materials 21 (6) (2005) 551–556.

[19] X. Guo, H. Yang, Effects of fluorine on crystallization, structure and performances of lithium aluminosilcate glass ceramic, Materials Research Bulletin 41 (2) (2006) 396–405.